DALTON
FULL PAPER

A vibrational spectroscopic, structural and quantum chemical study of the triiodide ion

Per H. Svensson [a] **and Lars Kloo** *[b]

[a] *Dipt. di Chimica Fisica ed Inorganica, Univ. di Bologna, Viale del Risorgimento 4, I-40136 Bologna, Italy*
[b] *Inorganic Chemistry, Royal Institute of Technology, S-100 44 Stockholm, Sweden*

Received 29th March 2000, Accepted 22nd May 2000
Published on the Web 30th June 2000

The vibrational spectra of $[R_3S]I_3$(l) (R = Me or Et) showed extra spectral features in the 145 and 170 cm^{-1} region, in contrast to what is predicted by the selection rules for I_3^- of $D_{\infty h}$ symmetry. Depolarisation experiments showed that the 170 cm^{-1} peak originates from a symmetric vibration mode. The addition of an excess of I^- obliterates the 170 cm^{-1} peak, whereas the peak at 145 cm^{-1} is invariant. The excess of I^- also introduces a decrease in intensity of the structural effects from I_3^- in the LXS reduced radial distribution function. The centrosymmetric polyhalide ions Br_3^- and IBr_2^- do not exhibit analogous spectral features to the triiodide ion. The results suggest that the extra spectral features observed for the triiodide systems are caused by the presence of higher polyiodides, *viz.* pentaiodides formed by the disproportionation reaction $2I_3^- \longrightarrow I_3(I_2)^- + I^-$, and a cation-induced, symmetry lowering of I_3^-. The results from the theoretical study support this showing that I_3^- and I_5^- have vibrational features in the 145 and 170 cm^{-1} region. The energy barrier to linear deformation is also shown to be very small both for linear and asymmetric triiodide ions, thus supporting the ideas about a Grotthus type of mechanism of conduction in polyiodides, where the triiodide ions act as iodide donors.

Introduction

Solid polyiodides have earned much attention due to the fact that they form low-dimensional materials with an electric conduction ranging from that of insulators to that of metals depending on their structure and composition.[1–3] Such properties obviously implicate technical applications in electronic and electrochemical devices.[4–7]

Apart from the potential technical importance of the polyiodide systems, they also exhibit an unusually rich structural chemistry. It should be emphasised that the polyiodide structures are one of the most common examples of homoatomic catenation or clustering. With very few exceptions, the structural entities can be divided into the fundamental and stable structural units I^-, I_2 and I_3^-. As can be observed in the structural fragments **a**, **b** and **c**, the local structures can be rationalised in standard co-ordination chemistry terms: the ions (I^- and I_3^-) are surrounded (solvated) by the neutral solvent molecules (I_2). Larger polyiodides are often networks, which have very different three-dimensional arrangement creating linear and zigzag chains as well as layers. Special interest has lately been devoted to polyiodides since they are one of the few classes of compounds that form extended anionic inorganic networks.[8–10] The question of whether to regard some of these structures as consisting of small discrete or large extended polyiodide anions depends of where the more or less arbitrary limit for what is regarded as an I–I interaction is set.[11]

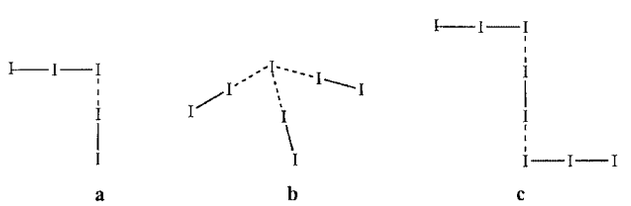

a **b** **c**

The rich diversity of polyiodide structures indicates that the possible orientations and configurations of the extended polyiodide structures are close in energy, and that small differences in counter ion, packing effects, iodine : iodide ratio or experimental conditions during synthesis have a large influence on the structure obtained.

Recently, polyiodides have received attention in template synthesis and molecular engineering.[9–12] In this context we have been using the $[R_3S]I_x$ (R = Me or Et; x = 2–11) systems as reaction media for the study and isolation of modified polyiodide networks.[13–15] The addition of iodide acceptors or metal iodides to an $(R_3S)I_x$ melt exposes the iodine to a competition for iodide ions. This enables the insertion of guest atoms into the polyiodide networks and thus modification of the I^--donating properties becomes possible. The knowledge of the fundamental physical properties of the $(R_3S)I_x$ reaction media is crucial in order to develop the synthesis of modified polyiodides. In the literature very few investigations are reported and a comprehensive interpretation of the spectroscopic vibrational features is lacking.

This work is based on a Raman and far-IR spectroscopic and X-ray diffraction investigation of molten and solid $[R_3S]I_x$ (R = Me or Et; x = 2–13) mixtures supported by a quantum chemical analysis of such systems. A Raman spectroscopic investigation of the analogous trihalide compounds $[Me_3S]Br_3$, $[Me_3S]IBr_2$, and $[Me_3S]I_2Br$ and the crystal structure of $[Me_3S]IBr_2$ are also included for sake of comparison. The consequences of our results for the vibrational properties and suggested electrical conductivity mechanism in polyiodides in general are also addressed.

Results and discussion

Crystal structures

The structure of $[Et_3S]I_3$, **1**, consists of pyramidal Et_3S^+ cations and the asymmetric (C_s) triiodide ions I(1)–I(2)–I(3) [I(1)–I(2) 2.951(4) and I(2)–I(3) 2.884(4) Å] and I(4)–I(5)–I(6) (nearly C_{2v}) [I(4)–I(5) 2.930(4) and I(5)–I(6) 2.932(4) Å] (Table 1). The former triiodide has an I–I–I angle of 174.6(1)°, while the latter

Table 1 Selected bond distances (Å) and angles (°) in compounds **1**, **2** and **3**

$[Et_3S]I_3$			
I(1)–I(2)	2.951(4)	I(5)–I(6)	2.932(4)
I(2)–I(3)	2.884(4)	I(1)···I(6)	3.879(4)
I(4)–I(5)	2.930(4)	I(2)···I(3)	3.998(4)
I(1)–I(2)–I(3)	174.6(1)	I(4)–I(5)–I(6)	179.2(1)
$[Me_3S]IBr_2$			
I(1)–Br(1)	2.7098(8)	I(2)···Br(1)	4.231(2)
I(2)–Br(2)	2.7098(8)		
Br(1)–I(1)–Br(1)	179.68(4)	Br(2)–I(2)–Br(2)	180
$[Me_3S]I_5$			
I(1)–I(2)	3.144(3)	I(2)···I(3)	3.791(4)
I(2)–I(3)	2.783(3)		
I(2)–I(1)–I(2)	86.3(1)	I(1)–I(2)–I(3)	173.7(1)

has an I–I–I angle of 179.2(1)°. These values correspond well to those found for other triiodide ions.[16] The I_3^- ions are packed as sheets, in which the ions are positioned so that T-shaped patterns arise.

The structure of $[Me_3S]IBr_2$, **2**, consists of pyramidal Me_3S^+ ions and Br–I–Br^- ions of C_{2v} [Br(1)–I(1)–Br(1)] and $D_{\infty h}$ [Br(2)–I(2)–Br(2)] symmetry. The I–Br distance is 2.7098(8) Å for both symmetries, while the Br–I–Br angle is 179.68(4)° for the C_{2v} ion. The IBr_2^- ions are packed in a pattern so that the terminal bromine points to the central iodide ion of a neighbouring anion, thus forming T-shaped arrangements. Notable is that the previously determined structure of the analogous $[Me_3S]I_3$ does not contain T-shaped patterns.[17] In both the compounds **1** and **2** the cation position is asymmetric with respect to the central iodine of the trihalides (see **e**).

The structure of $[Me_3S]I_5$, **3**, consists of pyramidal Me_3S^+ and planar, V-shaped (C_{2v}) I_5^- anions, which can be visualised as two I_2 units co-ordinating to one I^- unit $[I(I_2)_2^-]$. In this description the I_2 distance is 2.783(3) Å and the I_2–I^- distances are 3.144(3) Å (Fig. 1). The top angle is 86.33(10)° [I(2*)–I(1)–I(2)] and the I_2–I^- angle is 173.67(10)° [I(3)–I(2)–I(1)]. The pentaiodides are packed as sheets, which alternate in the directions of the diagonals in the *ab* plane (Fig. 1).

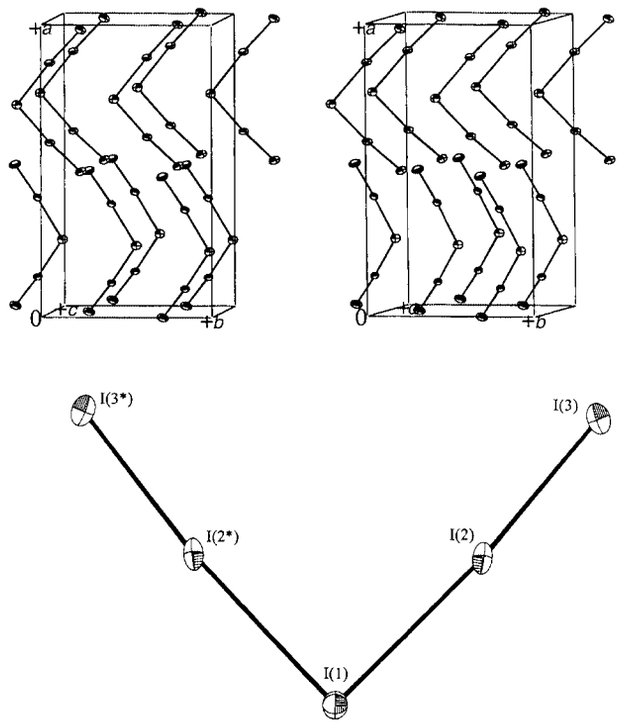

Fig. 1 Stereographic view of the crystal packing (cations are omitted for clarity) and ORTEP[18] view of the I_5^- anion in $[Me_3S]I_5$.

Vibrational spectroscopy and X-ray scattering

In a previous work[19] X-ray scattering experiments showed that the $[Et_3S]I_3$ melts consist of discrete, centrosymmetric I_3^- anions, **d**, and pyramidal Et_3S^+ cations. The cations co-ordinate

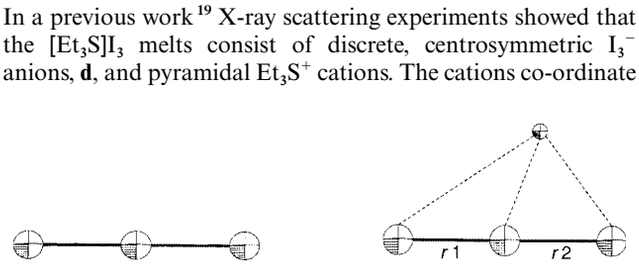

d **e**

asymmetrically to the triiodide ions at distances corresponding to the sum of the van der Waals (vdW) radii of S and I (1.80 and 2.15 Å), **e** (only the sulfur atom of the Et_3S^+ cation is shown).

The orientation of the hydrocarbon chains could not be distinguished. The melts containing more iodine can be described as consisting of ions (I_3^-) solvated by the neutral solvent molecules (I_2), very much in analogy with the features of solid polyiodides. The co-ordination geometry projected into two dimensions is shown in **f**, where the number of I_2 molecules co-ordinated to the central I_3^- increase with increasing I_2 concentration.

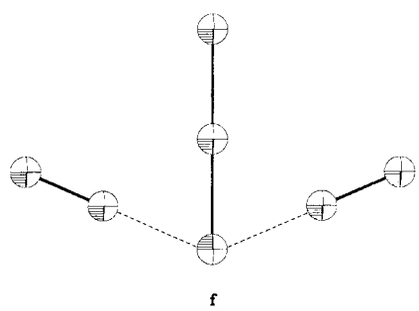

f

In a later study, the crystal structure of $[Me_3S]I_3$(s) was reported together with Raman spectra of the solid and molten compound.[17] The local structure and intermolecular I···S distances in the molten and solid state were shown to be analogous.

The Raman spectra of $[Et_3S]I_x$ (x = 3, 5, 7 or 11) and $[Me_3S]I_3$ are shown in Figs. 2 and 3 and the far-IR spectra of $[Et_3S]I_x$ (x = 3, 5 or 7) in Fig. 4. We will initially concentrate on the spectral features of the triiodide systems, since we believe that these display the fundamental vibrational spectroscopic properties of polyiodides. The selection rules for a centrosymmetric triiodide ion with $D_{\infty h}$ symmetry predict one Raman-active band from the centrosymmetric stretching vibration ($\nu_1 \approx 110$ cm^{-1}) and two IR-active bands from the antisymmetric stretching mode ($\nu_3 \approx 145$ cm^{-1}) and the bending mode ($\nu_2 \approx 75$ cm^{-1}, doubly degenerate). The Raman-active mode is IR forbidden and *vice versa*. As seen in Figs. 2–4, the Raman spectra of the molten triiodide systems exhibit additional bands in the region 130–170 cm^{-1}, while solid $[Me_3S]I_3$ follows the selection rules. The $[Et_3S]I_x$ melts, of formal $[Et_3S]I_x$ (x = 5, 7, 9 or 11) composition, produce an increase in intensity of the band at about 170 cm^{-1} relative to the band at 110 cm^{-1}. This band also shifts to higher wavenumbers until it reaches that of free iodine (approx. 180 cm^{-1}).[20,21] The far-IR spectrum also exhibits additional bands not expected for $D_{\infty h}$ symmetry (Fig. 4).

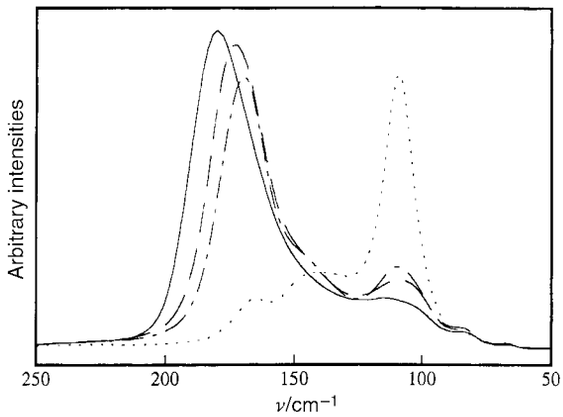

Fig. 2 The Raman spectra of molten $[Et_3S]I_3$ (---), $[Et_3S]I_5$ (—·—), $[Et_3S]I_7$ (— —) and $[Et_3S]I_{11}$ (——) at room temperature.

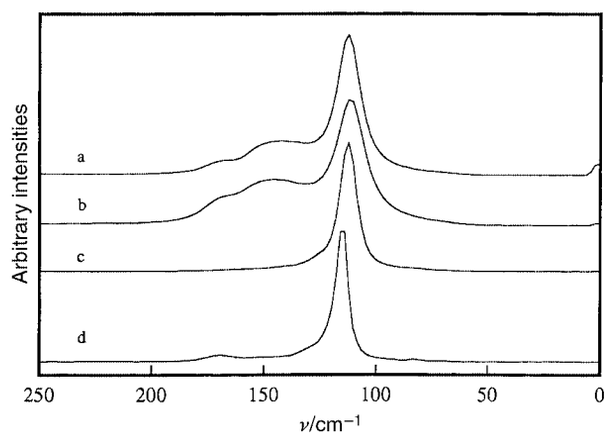

Fig. 3 The Raman spectra of (a) molten $[Et_3S]I_3$ at room temperature, (b) molten $[Me_3S]I_3$ at approximately 40 °C, (c) solid $[Me_3S]I_3$ at room temperature (mp = 37 °C) and (d) quenched $[Et_3S]I_3$ (−196 °C).

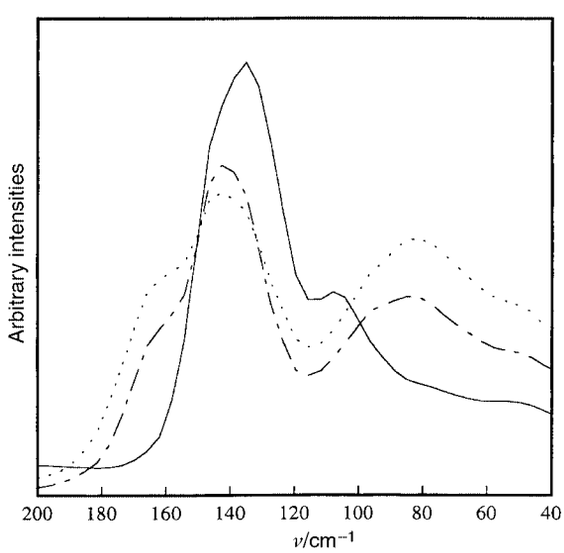

Fig. 4 The far-IR spectra of molten $[Et_3S]I_3$ (——), $[Et_3S]I_5$ (—·—) and $[Et_3S]I_7$ (---) at room temperature.

The vibrational bands in molten $[R_3S]I_x$ compounds are quite broad and overlapping, which makes the determination of the Raman depolarisation ratios difficult. The peaks at 110 and 170 cm^{-1} are clearly polarised, having depolarisation ratios of about 0.3 : 1, but the wide band at 145 cm^{-1} cannot adequately be characterised. However, information of interest can be extracted from the vibrational spectra of the newly isolated compound $[H_3O(dibenzo\text{-}18\text{-}crown\text{-}6)]I_5$(s), which consists of I_5^- units of asymmetric I_3^- interacting with I_2 [similar to liquid $[Et_3S]I_5$].[22] The Raman spectra exhibit three rather narrow bands analogous to those observed in the $[R_3S]I_x$ melts, where depolarisation experiments in solution show the bands at 110 and 170 cm^{-1} to be polarised and the central band to be depolarised.

The deviations from the expected spectra, based on the selection rules, for the trihalide systems have been observed before and there are various interpretations in the literature. Below, a survey of explanations suggested is presented and commented upon the basis of the spectroscopic results of this work.

Raman enhancement. Resonance-enhanced Raman spectroscopy has been used to produce spectral effects in polyiodide systems. The exciting laser beam has to be of the same wavelength, or nearly so, as the UV/vis absorption bands of the polyiodides.[23–26] Therefore, dramatic differences in Raman enhancement effects can be observed for the incident radiation wavelengths of 337.1 and 632.8 nm. Large effects are observed with a multitude of overtones for the former, and virtually no effects are observed for the latter. The UV/vis spectra of thin films of the $[Et_3S]I_x$ ($x = 3$, 5 or 7) melts all show strong electronic absorption bands below 650 nm. However, we have recorded identical Raman spectra of these polyiodides using both 647 and 1064 nm lasers. The latter wavelength is far away from any electronic spectral feature of the polyiodide systems studied here, and for this reason the extra vibrational bands at 130–170 cm^{-1} cannot be attributed to Raman enhancement effects. It should also be noted that the puzzling extra bands exist in the far-IR spectra as well.

Fermi resonance. It has been argued that the extra bands in both the far-IR and Raman spectra of the triiodides in solution are a result of Fermi resonance, much like that observed in the $D_{\infty h}$ molecules CO_2 and CS_2, in which the overtone of the bending mode couples with a stretching mode to produce extra spectral features.[27,28] Owing to the analogous local structure and intermolecular I · · · S distances in solid and liquid $[Me_3S]I_3$ this explanation is less likely: if the Fermi resonance is important, the effects should be observable in the spectra of both the solid and liquid compound. However, they are not. Therefore, Fermi resonance is not likely to be the cause of the additional spectral features under discussion.

Hot bands. The decrease in intensity of the peak at 140 cm^{-1} at low temperatures could be a result of changes in the population of excited vibrational states (giving rise to hot bands). However, since no peak suppression is seen at low temperatures, this is not a likely explanation. Furthermore, hot bands would be expected at lower wavenumbers (<110 cm^{-1}), rather than higher.

Artifacts caused by redox reactions. The $[R_3S]I_x$ melts have been shown to be stable at room temperature and elevated temperatures (373 K) for a considerable time. This indicates that no irreversible redox reaction or decomposition take place.

Dynamic process. A more exciting but less likely explanation would be to interpret the additional spectral features in the Raman and far-IR spectra of the molten trialkylsulfonium triiodide systems as a result of a dynamic process on the timescale of vibrational spectroscopy. The characteristic time of a vibration at 100 cm^{-1} is of the order of 10^{-13} s.

The Raman peaks at 110 and 170 cm^{-1} have Lorentzian lineshape and attempts to determine the lineshape of the central band were made. The basic idea being that the broad peak around 140 cm^{-1} is caused by the sampling of scattering from

Table 2 The results of geometry optimisations using different levels of electron correlation and the wavenumbers at about or above 100 cm^{-1}

Molecule	Method	I–I/Å		$\tilde{\nu}$/cm^{-1}		
I_2	HF	2.669		235		
	MP2	2.721		222		
	CCSD	2.745		210		
I_3^-	HF	2.984	2.984	119	104	62
	MP2	2.991	2.991	114	149	58
	CCSD	3.008	3.008	111	133	57
I_5^- [a]	HF	2.804	3.263	180(A_1)	164(B_2)	76(B_2)
	MP2	2.877	3.108	167(A_1)	146(B_2)	106(B_2)
	CCSD	2.874	3.172	164(A_1)	144(B_2)	84(B_2)

[a] V-shaped I_5^- ion of $I(I_2)_2^-$ type (C_{2v} symmetry).

many intermediate configurations between that of centrosymmetric I_3^- and asymmetric $I_2 \cdots I^-$, then the lineshape should be Gaussian rather than Lorentzian. However, the peak obtained after simulation and subtraction of the other peaks is equally well fitted by a Lorentzian and Gaussian model, simply because it is too broad to contain enough selective information in the tail regions also being affected by imperfections from the subtraction of the other two peaks.

Solvent effects. Recently it has been suggested that the presence of solvent can induce symmetry breaking of the triiodides.[29] The $[R_3S]I_3$ melts investigated in this paper are all formally without any solvent (unless you regard I_2 itself as the solvent) and consequently this explanation is analogous to the one suggesting the formation of higher polyiodides.

Disproportionation forming larger polyiodides. The additional bands at 145 and 170 cm^{-1} may be a consequence of a disproportionation of the triiodide ions in solutions or melts to higher polyiodides (*e.g.* I_5^- or I_7^-); $(n+1)I_3^- \longrightarrow I_3(I_2)_n^- + nI^-$. Larger formal polyiodides than I_7^- are not likely to exist at room temperature, considering the small cations and the liquid aggregation state in the sulfonium-based melts. Excess of I^- may of course give rise to species such as I_4^{2-} or I_6^{2-}. The previous results for molten trialkylsulfonium polyiodide melts are consistent with the formation of solvated triiodide ions, $I_3(I_2)_n^-$, where anions with $n = 1$ are the most probable initial decomposition product of the triiodide melts. This explanation also gains support from the fact that the extra spectral features are reduced in intensity upon the addition of I^-, thus reversing the disproportionation: $I_3(I_2)^- + I^- \longrightarrow 2I_3^-$.

The V-shaped pentaiodide ion shows vibrational bands both around 145 and 170 cm^{-1} (Table 2). The structural and spectroscopic properties (in the 145 and 170 cm^{-1} region) of the V-shaped (corresponding to $I(I_2)_2^-$; C_{2v} symmetry) and slightly distorted L-shaped (corresponding to $I_3^-(I_2)$; C_s symmetry) structure are very similar.[30] The results from the theoretical analysis are consistent with the experimental observations.

Theoretical data and recent results from the pentaiodide of protonated $[H_3O(dibenzo\text{-}18\text{-}crown\text{-}6)]I_5$(s), containing discrete $I_3(I_2)^-$ ions in the solid and liquid state, indeed show that a pentaiodide of both $I_3(I_2)^-$ and $I(I_2)_2^-$ type has significant vibrational peaks at about 170 and 145 cm^{-1}. The former peak arises from the symmetric stretch of an iodine molecule in a charge-transfer interaction, $I_2 \cdots I_3^-$ or $I_2 \cdots I^-$. The recent frequency–distance correlation by Deplano and co-workers is consistent with an intramolecular I–I distance of 2.75 Å.[31,32] The latter peak arises from the I_3^- unit, essentially corresponding to the asymmetric I–I stretch mode becoming Raman-active because of the lower symmetry. The experimental data for $[H_3O(dibenzo\text{-}18\text{-}crown\text{-}6)]I_5$(s) show that the intensity of the extra modes is of the same magnitude as that of the symmetric stretch mode of I_3^-.

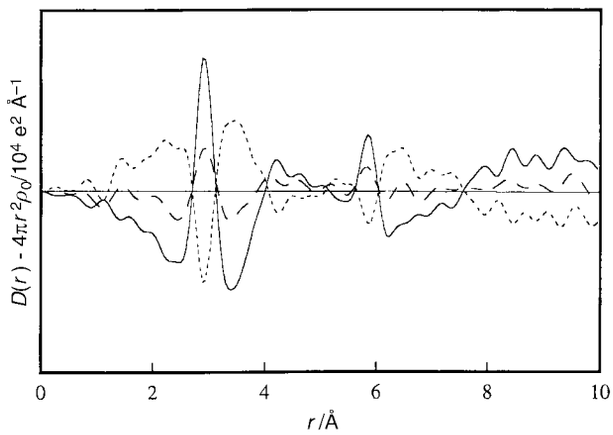

Fig. 5 Reduced RDFs of molten $[Et_3S]I_2$ (— —) and $[Et_3S]I_3$ (——) and their difference (– – –).

The liquid X-ray scattering data for the $[R_3S]I_3$ melts are consistent with an overall triiodide composition. However, a decomposition of 5–10% is not likely to heavily affect the rRDF (reduced radial distribution function) of these melts and could escape detection using this technique. However, vibrational spectroscopy, and Raman spectroscopy in particular, is a sensitive indicator for this phenomenon. A decomposition amounting to 5–10% could easily produce the extra spectral effects observed. A mass-spectroscopic analysis indicates that the triiodide melts consist of higher polyiodides (mainly I_5^-) to 5% or less.

Decomposition is thus a very likely explanation for the extra spectral features. However, one experimental observation indicates that additional effects may be of importance. The addition of I^- to an $[Et_3S]I_3$ melt indeed obliterates the extra peak at 170 cm^{-1}, but the peaks at 145 and 110 cm^{-1} remain. The rRDF of a melt of the formal composition $[Et_3S]I_2$ at 100 °C is essentially analogous to that of $[Et_3S]I_3$ (Fig. 5), although the structural features from the triiodide are weaker (lower concentration). These results seem to indicate that the extra vibrational peak at 145 cm^{-1} may consist of two separate contributions of which one is associated with the triiodide ion itself.

Cation co-ordination. Additional bands at about 130–170 cm^{-1} are observed in different solutions of triiodides with different cations.[20,23–25,27,32,35] Cations as different as K^+ and $N(n\text{-}Bu)_4^+$ produce, qualitatively, the same spectral effects. This may indicate a predominantly ionic cation–anion interaction. The I_3^-–Me_3S^+ distances are nearly the same in solid and liquid $[Me_3S]I_3$. Together with the long cation–anion distances observed it is therefore indicated that the interaction is mainly of Coulombic and vdW type. These speculations were verified by X-ray absorption spectroscopy, which shows that the cation–anion interaction does not contain any electron density.[17]

There is a large number of calculational studies at various levels of theory of iodine and polyiodides in the literature, but the bonding in the triiodide ion can in a simplified way be rationalised in terms of linear valence p-orbital interactions as originally proposed by Pimentel in 1951.[36] The bonding scheme can pedagogically visualised by using the extended Hückel formalism,[37] and is described by the σ-bonding/antibonding linear combinations of the valence 5p orbitals, but also involves contributions from the 5s orbitals. The bonding in I_2 and I_5^- (V or L shaped) can likewise be visualised in terms of valence I(5s) and I(5p) interactions. The bonding of triiodides was recently investigated by Hoffmann and co-workers[38] who confirmed the description made by Pimentel.

The reduced potential energy surfaces (PESs) of linear deformation of I_3^- obtained from HF, MP2 and CCSD calculations are extremely flat. This indicates a strong tendency to

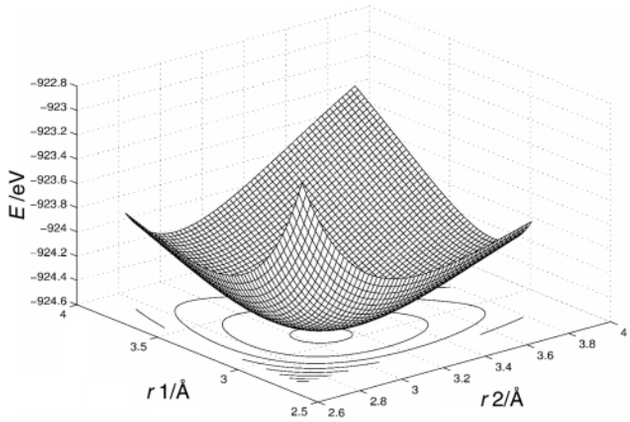

Fig. 6 Calculated energy of I_3^- as a function of $r1$ and $r2$ (MP2) [$r1$ and $r2$ are the intramolecular I–I distances in the triiodide, see **e**].

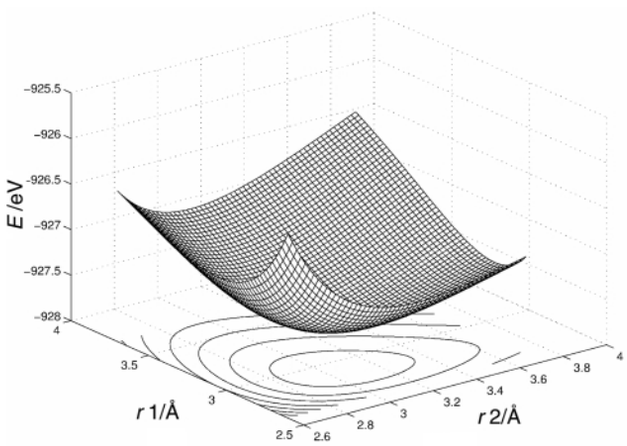

Fig. 7 Calculated energy of I_3^- as a function of $r1$ and $r2$ (MP2). Cation modelled by a point charge.

linear deformation (Fig. 6). The thermal energy at room temperature (kT) is about 0.025 eV, which would be enough to induce deformations as large as ≈0.3 Å. In view of the typical local structural arrangements in both liquid and solid polyiodide systems (**a** to **c**), this result highlights the I^--donor capacity of the triiodide ion in a Grotthus mechanism of electric conductivity, having a very low energy barrier. The angular deformation requires much higher energy. The inclusion of a cationic charge at the typical co-ordination site (see **e**) makes the reduced PES highly asymmetric (Fig. 7), thus reflecting the easy linear deformation induced by cation co-ordination and consequently the increased tendency of I_3^- to act as I^- donor.

The results of *ab initio* and extended Hückel calculations on a few tribromide and triiodide structures show that an asymmetric cation co-ordination mode, like that in **e**, is preferred and that it is sufficient to induce a distortion of the trihalide structure to $C_{\infty v}$ symmetry.[39]

The distortions of the triiodide ions in solid $[R_3S]I_3$, R = Me or Et, are not big enough to cause any strong extra peaks in the Raman and IR spectra. However, it is very possible that the process of melting the triiodide compounds is not only associated with a decomposition equilibrium forming higher polyiodides (*viz.* I_5^-), but also an ion-pairing equilibrium. The theoretical data cited above indicate a symmetry lowering upon cation interaction, and the appearance of an extra peak at about 145 cm^{-1} in the vibrational spectra can be explained at two levels: either using the correlation by Deplano *et al.* suggesting a deformation of the I_3^- ion to a shortest I–I distance of 2.85 Å, or an activation of the asymmetric stretch mode in the Raman spectra because of symmetry lowering. The introduction of bond asymmetry is thus not a necessary requirement for Raman activation of the asymmetric stretch vibration in I_3^-.

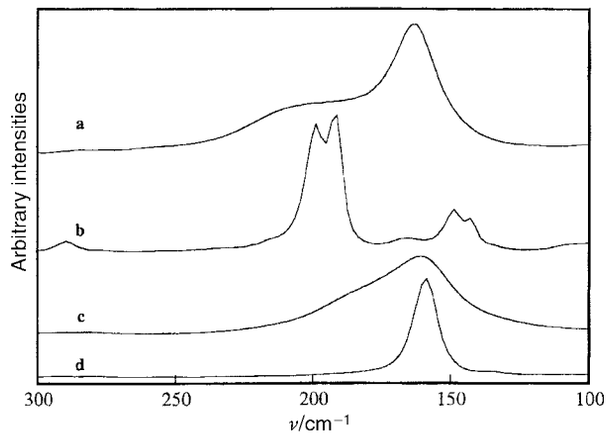

Fig. 8 The Raman spectra of (a) molten $[Me_3S]Br_3$ at room temperature, (b) solid $[Me_3S]Br_3$ (−196 °C), (c) molten $[Me_3S]IBr_2$ (85 °C) and (d) solid $[Me_3S]IBr_2$.

The present spectroscopic results thus imply that the 145 cm^{-1} peak appears because of a cation-induced, symmetry lowering of the I_3^- ion in the liquid state (ionic or molecular liquids).

Mixed trihalides. Additional information of relevance to the discussion above can be extracted from the structural and vibrational properties of the mixed Br/I trihalides.

The Raman spectrum of solid $[Me_3S]IBr_2$ shows a strong peak at 162 cm^{-1} which can be expected for the IBr_2^- ions of approximately $D_{\infty h}$ symmetry (Fig. 8).[33,34,40] The liquid $[Me_3S]IBr_2$ (85 °C) shows one broad peak at 161 cm^{-1} with a weak shoulder at 190 cm^{-1}. The Raman spectrum of liquid $[Me_3S]Br_3$ shows spectral features at 163 and 200 cm^{-1}, while for solid $[Me_3S]Br_3$ (quenched, −196 °C) peaks are seen at 144, 149, 166, 192, 199 and 290 cm^{-1}. The two pairs of narrow peaks (144, 149 and 192, 199 cm^{-1}) can be the result of isotope or factor group splitting.[34] Thus, the Raman spectra of $[Me_3S]I_3$ in the solid and liquid state are not equivalent to the symmetrically analogous $[Me_3S]IBr_2$ and $[Me_3S]Br_3$. Consequently, the extra spectral features are not an intrinsic property of the linear symmetry of the trihalide ions.

The I_2Br^- ion of $[Me_3S]I_2Br$ should be asymmetric (I–I–Br) and therefore have all three modes active in the Raman spectra. This is confirmed by the Raman spectrum of liquid $[Me_3S]I_2Br$, which displays peaks at 113, 140 and 169 cm^{-1}. The Raman spectrum of the solid $[Me_3S]I_2Br$ (quenched, −196 °C) also displays three peaks (117, 136 and 186 cm^{-1}). Asymmetry of the X_3^- unit thus is the prevailing explanation for the extra spectral features. However, the spectral features for $[Me_3S]I_2Br$ are observed at lower wavenumbers than expected. In addition, since the compound was only characterised by Raman spectroscopy further investigation will have to be undertaken in order to verify that the interhalogen species present is really I_2Br^- (I–I–Br^-).

Concluding remarks

The results from the spectroscopic and liquid X-ray scattering (LXS) experiments on the $[R_3S]I_3$ systems strongly suggest the extra Raman bands are caused by two effects, one chemical and one physical. Chemically, the presence of higher polyiodides, *e.g.* pentaiodides of $I(I_2)_2^-$ or $I_3^-(I_2)$ configuration as emerging from the disproportionation $2I_3^- \longrightarrow I_3(I_2)^- + I^-$, give rise to bands at both 145 and 170 cm^{-1}. Physically, the broad band in the 145 cm^{-1} region is caused by symmetry lowering from cation co-ordination of I_3^- making the asymmetric stretch vibration Raman active. The latter effect does not necessarily imply a difference in the two I–I distances in I_3^-, although the energy of linear deformation is extremely low (at the magnitude

of thermal energy at room temperature). This observation supports a Grotthus mechanism of conductivity in polyiodides, where I_3^- ions are almost invariably surrounded (solvated) by I_2 molecules that can readily act as I^- acceptors.

Experimental

Chemicals

The $[R_3S]I_x$ (R = Me or Et) compounds were prepared from the corresponding $[R_3S]I$ salts (Lancaster) and iodine (Merck, *p.A.*) by direct reaction of the stoichiometric amounts. $[Me_3S]IBr_2$ was prepared from the reaction of stoichiometric amounts of $[Me_3S]I$ and bromine (Merck, *p.A.*) in ethanol, $[Me_3S]Br_3$ from stoichiometric amounts of $[Me_3S]Br$ and bromine and $[Me_3S]I_2Br$ from stoichiometric amounts of $[Me_3S]Br$ and iodine in ethanol. The synthesis of $[Me_3S]Br$ has been described elsewhere.[41] The trialkylsulfonium iodides were purified by recrystallisation from hot ethanol before use.

UV/Vis Spectroscopy

The UV/vis spectra of thin films of the $[Et_3S]I_x$ ($x = 3$, 5 or 7) melts were recorded by a Guided Wave Model 260 fiber optics spectrometer with mercury and deuterium lamps, and PMT and silicon detectors in order to cover the spectral range between 200 and 1100 nm.

Vibrational spectroscopy

The far-infrared (far-IR) spectra were recorded on a Bio-Rad FTS 6000 FT-IR spectrometer using a resolution of 8 cm^{-1}. A Globular light source was used and a 6.25 μm Mylar beamsplitter in combination with a PE-DTGS detector produced an effective spectrum range of 50–550 cm^{-1}. The window material was polyethylene of spectroscopic quality (Merck). The backscattering of the $[R_3S]I_x$ melts and solids was recorded using the 1064 nm radiation from an Nd:YAG laser in a Bio-Rad FT-Raman spectrometer. The radiation was recorded using a nitrogen-cooled, Ge-diode detector with 4 cm^{-1} resolution. The Raman spectra of the $[Me_3S]IBr_2$ melt (85 °C) and $[Et_3S]I_2$ melt (100 °C) were recorded on a Bruker IFS-66/FRA-106 FT-Raman spectrometer with 4 cm^{-1} resolution.

Mass spectroscopy

The mass spectra of the $[R_3S]I_x$ (R = Me or Et, $x = 3$–11) melts were recorded on a JEOL SX-102 spectrometer. The methods used were FAB, CI and EI.

X-Ray diffraction

Crystals of $[Me_3S]IBr_2$ **2** were grown at room temperature by slow evaporation from an ethanol solution. Those of $[Et_3S]I_3$ **1** and $[Me_3S]I_5$ **3** were obtained at 193 K from an acetone–polyiodide solution. They were mounted on a glass fibre at approximately 193 K and stored in liquid nitrogen until mounted at the diffractometer. A summary of the crystallographic data is provided in Table 3. All data were corrected for Lorentz-polarisation effects and an empirical absorption correction was applied using the ψ-scan (compounds **1** and **3**) and SADABS (**2**) methods.[42,43] The structures were solved by the direct methods of SIR 92 (**1**) and SHELXTL PLUS (**2** and **3**).[44–46] The carbon atoms of the cation in **1** were refined isotropically owing to high thermal motion. The sulfur atom of the cation in **3** has a twofold disorder and the cation atoms of **3** were refined isotropically owing to high thermal motion. Hydrogen atoms were put in calculated positions in compounds **1** and **2**. The structure of **1** was refined on $|F|$, while those of **2** and **3** were refined on $|F|^2$.

CCDC reference number 186/2006.

See http://www.rsc.org/suppdata/dt/b0/b002492i/ for crystallographic files in .cif format.

Table 3 Crystallographic data for $[Et_3S]I_3$ **1**, $[Me_3S]IBr_2$ **2** and $[Me_3S]I_5$ **3**

	1	**2**	**3**
Formula	$C_6H_{15}I_3S$	$C_3H_9Br_2IS$	$C_3H_9I_5S$
M	499.96	363.88	711.66
Space group	*Pnma*	*C*2/*c*	*Ama*2
Crystal system	Orthorhombic	Monoclinic	Orthorhombic
Z	8	8	4
a/Å	9.894(2)	15.0570(8)	15.841(2)
b/Å	13.846(3)	9.7571(5)	9.334(1)
c/Å	19.856(6)	14.9825(8)	9.363(2)
β/°		115.99(3)	
V/Å^3	2719(1)	1978.4(2)	1384.3(3)
Z	8	8	4
D_c/g cm^{-3}	2.441	2.443	3.415
μ/cm^{-1}	70.03	114.44	113.3
T/K	150	293	150
Unique data	2725	1942	585
Observed data	1320 [$>3\sigma(I)$]	1454 [$>2\sigma(I)$]	308 [$>2\sigma(I)$]
R (R_w) (%)	6.66 (7.74)	3.97[a] (9.13[b])	4.55[a] (11.60[b])

[a] $R1(F)_{obs}$. [b] $R_w(F^2)_{obs}$.

Liquid X-ray scattering

The liquid structure of the formal $[Et_3S]I_2$ melt was investigated at 100 °C. The melt was kept in a capillary inside a furnace with a closed compartment and a 0.001 mm aluminium window. The measurements were performed on a Seifert GSD θ-θ diffractometer using Mo-Kα radiation. The intensity of the scattered radiation from the capillary was detected at discrete scattering angles using an EG&G ORTEC germanium solid state detector, in which the photon energy discrimination was adjusted electronically. Corrections were made for polarisation, Compton scattering and background radiation. The data treatment has previously been described in detail.[47]

Computations

The results presented in this work emerge from Hartree–Fock calculations at different levels of sophistication employing the GAUSSIAN 94 program package.[48] Both old and new and more sophisticated methods of calculation and basis sets were reviewed in order to find a proper basis set, preferably including effective core potentials (ECPs) minimising the computational effort. A (7s7p1d)/[3s3p1d] valence basis set and quasi-relativistic ECP was found to be appropriate for the qualitative or semi-quantitative information needed in this work.[49]

Dynamic electron correlation effects are not expected to be significant in molecules such as polyiodides, but calculations using the 2nd-order Møller–Plesset perturbation (MP2) and the coupled cluster method including single and double excitations (CCSD) were employed in order to check this explicitly.

Acknowledgements

The Swedish Natural Science Research Council is acknowledged for its financial support and the NSC at Linköping University and PDC at the Royal Institute of Technology in Stockholm for the allocation of computer time.

References

1 P. Coppens, in *Extended Linear Chain Compounds*, ed. J. S. Miller, Plenum Press, New York, 1982, vol. 19, p. 333.
2 T. J. Marks and D. W. Kalina, in *Extended Linear Chain Compounds*, ed. J. S. Miller, Plenum Press, New York, 1982, vol. 1, p. 197.
3 K.-F. Tebbe, in *Homoatomic Rings, Chains and Macromolecules of Main-Group Elements*, ed. A. L. Rheingold, Elsevier, Amsterdam, 1977, p. 551.
4 H. Stegemann, G. Jabs, H. Mittag, L. Schmidt, H. Füllbier, P. Cikmas, G. Petrovskis, G. Lusis and A. S. Orliuks, *Z. Anorg. Allg. Chem.*, 1987, **555**, 183.

5 B. B. Owens, B. Pate, P. M. Skarstad and D. L. Worburton, *Solid State Ionics*, 1983, **9/10**, 1241.
6 E. Falques, P. Molinre, P. Berdahl, T. P. Nguyen and J. Mansot, *Physica*, *Ser. C*, 1994, **219**, 297.
7 W. R. Salaneck, H. R. Thomas, R. W. Bigelow, C. B. Duke, E. W. Plummer, A. J. Heeger and A. G. Macdiarmid, *J. Chem. Phys.*, 1980, **73**, 4746.
8 K.-F. Tebbe and R. Buchem, *Angew. Chem.*, 1997, **109**, 1403; *Angew. Chem.*, *Int. Ed. Engl.*, 1997, **37**, 1345.
9 A. J. Blake, R. O. Gould, S. Parsons, C. Radek and M. Schröder, *Angew. Chem.*, 1995, **107**, 2563; *Angew. Chem.*, *Int. Ed. Engl.*, 1995, **34**, 2374.
10 A. J. Blake, R. O. Gould, W.-S. Li, V. Lippolis, S. Parsons, C. Radek and M. Schröder, *Angew. Chem.*, 1998, **110**, 305; *Angew. Chem.*, *Int. Ed.*, 1998, **37**, 293.
11 M. Bittner, *Präperative und röntgenographische Untersuchungen an Polyiodiden von 2,2′-Bipyridin*, Ph.D. Thesis, Köln, 1994.
12 R. D. Bailey, L. L. Hook and W. T. Pennington, *Chem. Commun.*, 1998, 1181.
13 H. Stegemann, K.-F. Tebbe and L. A. Bengtsson, *Z. Anorg. Allg. Chem.*, 1995, **621**, 165.
14 P. H. Svensson, L. Bengtsson-Kloo and P. Persson, *J. Chem. Soc.*, *Dalton Trans.*, 1998, 1425.
15 P. H. Svensson, J. Rosdahl and L. Bengtsson-Kloo, *Chem Eur. J.*, 1999, **5**, 305.
16 Cambridge Structural Database System, Database V. 5.14, Cambridge, 1997; Inorganic Structural Database ICSD, Gmelin Institut, 1998.
17 L. A. Bengtsson, Å. Oskarsson, H. Stegemann and A. Redeker, *Inorg. Chim. Acta*, 1994, **215**, 33.
18 C. K. Johnson, ORTEPII, Report ORNL-5138, Oak Ridge National Laboratory, Oak Ridge, TN, 1976.
19 L. A. Bengtsson, H. Stegemann, B. Holmberg and H. Füllbier, *Mol. Phys.*, 1991, **73**, 283.
20 P. Deplano, F. A. Devillanova, J. R. Ferraro, F. Isaia, V. Lippolis and M. L. Mercuri, *Appl. Spectrosc.*, 1992, **46**, 1625.
21 J. S. Zambounis, E. I. Kamitsos, A. P. Patsis and G. C. Papavassiliou, *J. Raman Spectrosc.*, 1992, **23**, 81.
22 L. Kloo, P. H. Svensson and M. J. Taylor, *J. Chem. Soc.*, *Dalton Trans.*, 2000, 1061.
23 K. Kaya, N. Mikami, Y. Udagawa and M. Ito, *Chem. Phys. Lett.*, 1972, **16**, 151.
24 W. Kiefer and H. J. Bernstein, *Chem. Phys. Lett.*, 1972, **16**, 5.
25 M. E. Heyde, L. Rimai, R. G. Kilponen and D. Gill, *J. Am. Chem. Soc.*, 1972, **94**, 5222.
26 W. F. Howard and L. Andrews, *J. Raman Spectrosc.*, 1974, **2**, 447.
27 J. Milne, *Spectrochim. Acta*, *Part A*, 1992, **48**, 533.
28 G. Herzberg, *Molecular Spectra and Molecular Structure, Part II, Infrared and Raman Spectra*, van Nostrand, Princeton, 1966.
29 H. Sato, F. Hirata and A. B. Myers, *J. Phys. Chem.*, 1998, **102A**, 2065.
30 J. Rosdahl, Diploma work, *How to Insert the Gold Iodide Complexes AuI_2^- and AuI_4^- into Polyiodide Networks*, Lund University, 1997.
31 P. Deplano, F. A. Devillano, J. R. Ferraro, M. L. Mercuri, V. Lippolis and E. F. Trogu, *Appl. Spectrosc.*, 1994, **48**, 1236.
32 S. G. W. Ginn and J. L. Wood, *Chem. Commun.*, 1965, 262.
33 A. G. Maki and R. Forneris, *Spectrochim. Acta*, *Part A*, 1967, **23**, 867.
34 W. Gabes and H. Gerding, *J. Mol. Struct.*, 1972, **14**, 267.
35 J. R. Ferraro, K. Martin, A. Furlani and M. V. Russo, *Appl. Spectrosc.*, 1984, **38**, 267.
36 G. C. Pimentel, *J. Chem. Phys.*, 1951, **19**, 446.
37 J. J. Novoa, F. Mota, M.-H. Whangbo and J. M. Williams, *Inorg. Chem.*, 1991, **30**, 54.
38 G. A. Landrum, N. Goldberg and R. Hoffmann, *J. Chem. Soc.*, *Dalton Trans.*, 1997, 3605.
39 J. J. Novoa, F. Mota and S. Alvarez, *J. Phys. Chem.*, 1988, **92**, 6561.
40 G. C. Hayward and P. J. Hendra, *Spectrochim. Acta*, *Part A*, 1967, **23**, 2309.
41 P. H. Svensson and L. Kloo, *Acta Crystallogr.*, *Sect. C*, 1996, **52**, 2580.
42 A. C. T. North, D. C. Phillips and F. S. Mathews, *Acta Crystallogr.*, *Sect. A*, 1968, **24**, 351.
43 SADABS, G. M. Sheldrick, Program for Absorption Correction, University of Göttingen, 1996.
44 A. Altomare, M. C. Burla, M. Camalli, M. Cascarano, C. Giacovazzo, A. Guagliardi and G. Polidori, *J. Appl. Crystallogr.*, 1994, **27**, 435.
45 TEXSAN, Crystal Structure Analysis Package, Molecular Structure Corporation, Houston, TX, 1985 and 1992.
46 SHELXTL PLUS, G. M. Sheldrick, Siemens Analytical Instruments, Madison, WI, 1992.
47 S. Ulvenlund and L. A. Bengtsson, *J. Mol. Struct.*, 1994, **326**, 181.
48 GAUSSIAN 94, Revision B.3, M. J. Frish, G. W. Trucks, H. B. Schlegel, P. M. W. Gill, B. G. Johnson, M. A. Robb, J. R. Cheeseman, T. A. Keith, G. A. Petersson, J. A. Montgomery, K. Raghavachari, M. A. Al-Laham, V. G. Zakrzewski, J. V. Ortiz, J. B. Foresman, J. Cioslowski, B. B. Stafanov, A. Nanayakkara, M. Challacombe, C. Y. Peng, P. Y. Ayala, W. Chen, M. W. Wong, J. Andres, E. S. Replogle, R. Gomperts, R. L. Martin, D. J. Fox, J. S. Binkley, D. J. Defrees, J. Baker, J. P. Stewart, M. Head-Gordon, C. Gonzales and J. A. Pople, Gaussian Inc., Pittsburg, PA, 1995.
49 P. Schwerdtfeger, M. Dolg, W. H. E. Schwarz, G. A. Bowmaker and P. D. W. Boyd, *J. Chem. Phys.*, 1989, **91**, 1762.